RJC

RASĀYAN *J. Chem.*
Vol. 17 | No. 3 |1242-1250| July - September | 2024
ISSN: 0974-1496 | e-ISSN: 0976-0083 | CODEN: RJCABP
http://www.rasayanjournal.com
http://www.rasayanjournal.co.in

EFFECT OF Na_2O ON THE ENHANCEMENT OF ELECTRICAL CONDUCTIVITY, STRUCTURAL, AND OPTICAL PROPERTIES OF BORATE BASED GLASSES CONTAINING BaO AND ZnO FIXED MODIFIERS FOR SOLID STATE ELECTROLYTE APPLICATIONS

Jagram Anterbedy[1], Pallati Naresh[2], Aravind Seema[1], A. Rajesh[1] K. Santosh Kumar[3] and Gangadhar Thalari[1,✉]

[1]Department of Chemistry, Osmania University, Hyderabad-500007, Telangana, India
[2]Department of Physics, UCS Saifabad, O.U, Hyderabad-500004, Telangana, India
[3]Department of Chemistry, Geetanjali College of Engineering and Technology, Cheeryal Hyderabad-501301, Telangana, India
✉Corresponding Author: gangadharchemou@gmail.com

ABSTRACT

A glass series synthesized with composition $(Na_2O)_x.(ZnO)_{10}.(BaO)_{10}.(B_2O_3)_{80-x}$ as x=0-20mol% for the AC conductivity analysis concerning temperature and frequency. The incorporation of Na_2O, results in enhancing AC conductivity up to two orders in both low frequency and high frequency. The Cole-Cole impedance plots exhibited semi-circles with a decrease in the radius, which reveals the decreasing bulk resistance values of the glass samples at higher temperatures. The results of AC conductivity and Cole-Cole plots were matched with the nearest AC conduction values. The FT-IR spectrum confirmed the role and structural variations of network modifiers due to the addition of Na_2O. The optical spectroscopy resulted in an increase in cut-off, a decrease in band gaps, an increase in refractive index, and Urbach energy. The density increased & molar volume decreased with Na_2O content. The higher order conductivity (10^{-3} ohm^{-1} cm^{-1}) confirms the suitability of the glasses for battery and solid-state electrolytes.

Keywords: AC Conductivity, Space-Charge Polarization, Bulk Resistance, BO_4 Units, Density, Optical Band-Gap.
RASĀYAN *J. Chem.*, Vol. 17, No.3, 2024

INTRODUCTION

Borate-based inorganic oxide glasses are familiar with their transparency, chemical durability, and thermal stability and also due to the variety of structural units along with BO_3 and BO_4 units.[1] The metal oxide doped borate glasses cause the enhancement of properties like anti-bacterial efficiency, conductivity, and optical features because of the non-bridging oxygens.[2] The metal oxide dopant inserts into the borate glass network and transforms the original network. In recent days, the borate glasses also exhibited radiation shielding applications due to higher densities when it is doped with heavy metal oxides. BaO-containing borate glasses are useful in optical device applications. The role of BaO and ZnO is as network modifiers in the glass matrix. ZnO is also an element of higher refractive index and density. Basically, ZnO is a semiconductor which widely used as a photocatalyst due to its higher activity, eco-friendliness low price and also more availability. The role of ZnO in the glass networks is a modifier incorporated into the structure in the form of a divalent Zn^{+2} ion. Enrichment of ZnO into glass networks results in the enhancement of optical features, improvement of conductivity, upgradation of structural variation, and also raising in the zone of inhibition in bio-activity.[3] Na_2O acts like a modifier and the addition of Na_2O into borate glass decreases the melting points of the glass networks. The reason behind the decrement is the formation of the basic crystalline phase and the breakage of the actual crystalline phase. The study of AC conductivity is very useful in the extraction of information about the different dielectric relaxation mechanisms. Different materials show different energy band gaps which can be used for the classification of materials based on their conductivity. Basically, conductivity is classified into two i.e. AC Conductivity (frequency dependent) and DC conductivity (temperature dependent). In the FTIR

http://doi.org/10.31788/RJC.2024.1738851
This work is licensed under a CC BY 4.0 license.

study, the molecules absorb infrared light and get excited. The absorption spectrum is produced from photon transitions. The many modes of vibrational frequencies resulting from molecular bonding identified in the sample show the presence of inorganic substances and chemical bonds. This technique allows for both quantitative and qualitative analysis of glass samples. It has the ability to identify covalent bonds between atoms as well. Radiation shielding efficacy of the zinc-lithium-borate glasses was theoretically studied with different molar fractions of additive content and proved that the increasing values of alkali additive causes the enhancement of photon-absorption efficiency and also used as radiation protection functions.[4.] An investigation was done for the energy storage capacity of Borate glasses containing ZnO and concluded that the ac conductivity enhanced with different metal oxide modifiers etc. The estimated activation energies were found in the range of 0.89eV to 1.39eV. The ac conduction, structural, and physical along with optical properties on borate glasses reveal their efficiency, and enhanced properties with different network modifiers were reported by researchers recently. The energy density, storage capacity, movement of cations, and suitability of solid-state batteries were reported.[5] The aim of the investigation is to examine the effect of Na_2O on the ac conductivity, structural variations, optical features, and also the variations in the density-based parameters with clear differentiation as a function of the alkali network modifier Na_2O. The major contribution of the cations and their role along with NBOs, in the properties changes have been discussed in detail. The role of Na^+in the enhancement of ac conductivity is also discussed for the suitability of the present synthesized glasses for battery, solid-state electrolytes, and energy storage device applications.

EXPERIMENTAL

Material and Methods

A conventionally familiar melt-derive route was adopted for the synthesis of the glasses. The oxide forms of the chemical compositions were selected as the starting elements. The stoichiometric ratios were fixed and the required amount of oxides was weighted on Dona balance with an accuracy of 0.0001g. The starting chemical oxides were mixed in a crucible made up of platinum for re-usage and inserted into the electrical furnace already maintained at 1055ºC. Within 30min the powder mixture was melted and the solution was stirred thoroughly for uniformity. It was poured onto the metal plate maintained at 250ºC and quenched rapidly. Different shapes of glass samples were prepared using different metal molds with different dimensions for further studies. Finally, the prepared glassy materials were exposed to the annealing process in the removal of various strains. The characteristics of the glassy amorphous solids were analyzed using different techniques. The non-crystalline behavior of the glass series confirmed with the X-ray diffraction method in Bragg's angle ranged from 10º-80º. The AC conductivity measurements were done from room temperature to 400Oc in the frequency range from 5Hz to 35MHz with a step variation of 50ºC. The IR and Raman measurements were carried in the wavenumber range 250-4000-1 and 200-2000cm^{-1}respectively. The optical characteristics of the glass series were analyzed in the wavelength of 200-1000nm at room temperature and density studies were done from the Archimedes principle.

RESULTS AND DISCUSSION

Glassy Nature Confirmation Study with XRD

The prepared transparent glassy samples were scanned for the determination of amorphous character using an X-ray diffractometer. The short-range order and also non-periodicity are found in the glasses. There was no crystalline (sharp) peaks were found in the patterns of XRD for all the Na2O-enriched glassy compositions. The characteristic features of the amorphous behavior of glasses were found due to the presence of broad humps near the Braggs angle 26º-29º in the XRD spectra.[6] The intensity of the XRD patterns is almost stable with an addition of Na_2O into the glass matrix. The patterns of X-ray scanning of sodium oxide Na_2O series are shown in Fig.-1. With different scan rates also no changes were found in the XRD spectra. We can conclude that the effect of the rate of scan on the XRD result is ignorable.

AC Conductivity in Terms of Frequency and Temperature

The analysis of AC conductivity is an advantageous technique over the other methods of electrical conductivity. AC conductivity deals with the transportation of charge carriers from one site to another site

in a particular direction with an application of an external electric field. The applied field affects the excitation of the atoms of the solids like crystalline materials, non-crystalline materials, etc. Even, the glasses are non-crystalline amorphous, and exhibit conductivity up to a satisfactory range. The frequency also influences the order of AC conductivity as charge carriers polarize into the direction of external electric field. Due to the cationic moment in the localized structures, the order of conductivity may arise. It may be studied and analyzed with the support of Jonscher power law with a frequency exponent as follows.

$$\sigma_{AC} = 2\pi f \varepsilon' \varepsilon_0 tan\delta \qquad (1)$$

The compositional variation of ac conductivity has been analyzed with the incorporation of Na_2O into the ZnO-BaO-B_2O_3 glass network. The entry of network modifier Na_2O results in the accumulation of Na^+ ions which leads to the free moment of cations due to the presence of NBOs in the glass network. In the low-frequency domain, the order of ac conduction was found the lowest when compared to the high-frequency region. Due to the increment in the frequency, the charge carriers try to lie in the field direction, therefore, the orientation of the ions improved i,e polarized. The jumping of ions takes place in the high-frequency domain, therefore higher order of conductivity results was found. Lower-order conductivity is found with lower temperatures due to the existence of impurities or inhomogeneity in the glassy sample.[7] The order of conductivity is enhanced by raising the temperatures because of bond breakages and the liberty of the ions. The behavioural changes of AC conductivity concerning the temperature as well as the frequency of pure sample (Na-0) are shown in Fig.-2. Pure sample in which there is no presence of Na cations, but due to the presence of Zn^{+2} cations, Ba^{+2} the order of ac conductivity σ_{ac} is $10^{-8}\Omega^{-1}cm^{-1}$ at 100^0C. By increasing the temperature up to 400ºC it was improved to $10^{-6}\Omega^{-1}cm^{-1}$ in the lower frequency domain. σ_{ac} was found to be $10^{-6}\Omega^{-1}cm^{-1}$ at 100^0C and improved to $10^{-4}\Omega^{-1}cm^{-1}$ at 400^0C in the high-frequency domain. It might be due to the space-charge polarization mechanism taking place.[8] The overall variation conductivity in the sample is by two orders in both the regions with respect to the temperature and applied frequency. The behavioural changes of AC conductivity concerning the temperature as well as frequency of the Na-5 sample are shown in Fig.-3. The starting entry of sodium oxide into a base glass (Na-5), results in the variation of ac conductivity, due to Na^+, Zn^{+2} cations, and Ba^{+2} ions. The order of ac conductivity σ_{ac} is $10^{-7}\Omega^{-1}cm^{-1}$ at 100^0C. By increasing the temperature up to 350ºC it was improved to $10^{-5}\Omega^{-1}cm^{-1}$ in the lower frequency domain. σ_{ac} found to be $10^{-5}\Omega^{-1}cm^{-1}$ at 100^0C and improved to $10^{-4}\Omega^{-1}cm^{-1}$ at 350^0C in the high frequency domain. It might be due to the similar mechanism taking place in the glassy sample. The overall variation conductivity in the sample is by two orders in both regions with respect to the temperature and applied frequency. Na-10 and Na-15 samples also exhibited similar results of ac conductivity by two orders. The behavioural changes of AC conductivity with respect to the temperature as well as the frequency of the Na-20 sample are shown in Fig.-4. The highest sodium oxide Na_2O containing (Na-20) has shown the highest ac conductivity due to the high population density of cations in the form of more Na^+. For this sample, the variation in the ac conductivity is only one order, but, the highest. The order of ac conductivity σ_{ac} is $10^{-5}\Omega^{-1}cm^{-1}$ at 100^0C. By increasing the temperature up to 350ºC it was improved to $10^{-4}\Omega^{-1}cm^{-1}$ in the lower frequency domain. σ_{ac} was found to be $10^{-4}\Omega^{-1}cm^{-1}$ at 100^0C and improved to $10^{-3}\Omega^{-1}cm^{-1}$ at 350^0C in the high-frequency domain. It might be due to a similar mechanism. The overall variation conductivity in the sample is in one order.

Cole-Cole Impedance Characteristics of Na_2O Enriched Into Zinc-Barium-Borate Glasses

The components of impedance in its real and imaginary can be analyzed as

$$Z' = \frac{G}{(G^2+\omega^2C^2)} \qquad (2)$$

$$Z'' = \frac{\omega C}{(G^2+\omega^2C^2)} \qquad (3)$$

G-Conductance, ε' – permittivity in air and ε_0 -permittivity of free space, C-capacitance, tan δ-dielectric loss tangent, $Z^{'}$ - impedance component of real part & $Z^{''}$-imaginary impedance. The impedance behavior of the BZBNa glass series at changing temperatures has been discussed here. The variations of $Z^{/}$ vs. $Z^{//}$

parts as shown in the figures Fig.-5 (a-c). In the plots drawn between real and imaginary components of the impedance of Na_2O enriched into borate base glasses have shown a single semicircle at higher temperatures. The bulk resistance has been calculated from the x-intercept of the Cole-Cole plots. It decreases with increasing temperature, which is an indication of increasing trends of AC conductivity. The Cole-Cole impedance results were good at 200°C, 250°C, 300°C and 350°C. Due to the sample-electrode interface, the results at lower temperatures are not good.

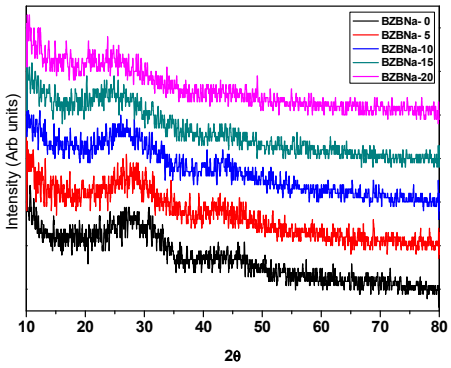

Fig.-1: XRD Spectra of the Glass System

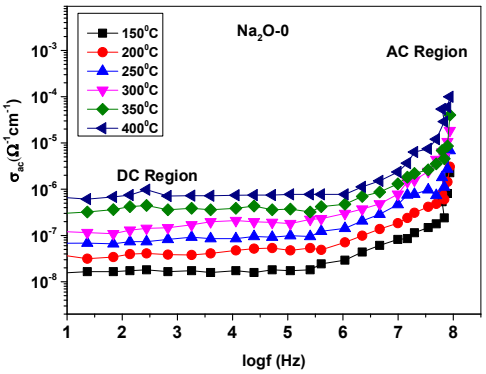

Fig.-2: variation of σ_{ac} of Na_2O-0 Sample

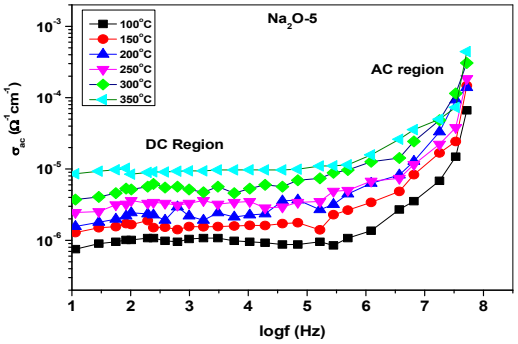

Fig.-3: Variation of σ_{ac} of Na_2O-5 Sample

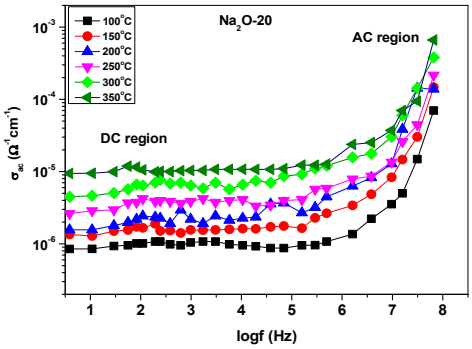

Fig.-4: Variation of σ_{ac} of Na_2O-20 Sample

The pure sample has shown the bulk resistance in the order of 10^7ohm, further, it was decreased to numerical values in the same order. Increasing values of the modifier sodium oxide, results in the decrease of bulk resistance.[9] The starting entry of sodium oxide into base glass (Na-5), results in the change of bulk resistance with decreased values in the order of 10^6 ohm. One more order of bulk resistance decreased for more addition of sodium oxide for Na-10 and Na-15 samples which were shown 10^6 ohms and 10^5ohm respectively. Finally, the highest Na-containing Na-20 sample has given the lowest values of bulk resistance in the order of 10^4ohm. The lowest R_b means that it exhibits the highest order of conductivity.

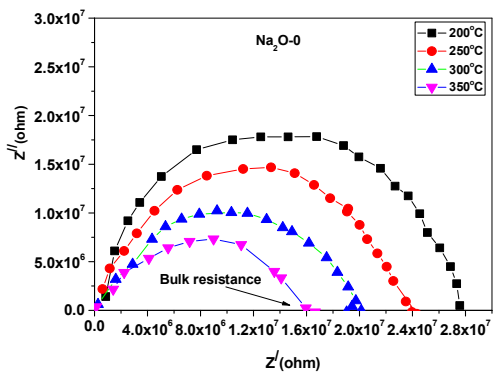

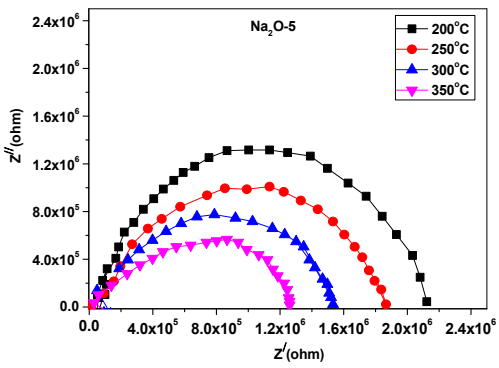

Fig.-5:(a-b) The Cole-Cole Impedance Plots of Na_2O-0 and Na_2O-5 Incorporated Glass Series

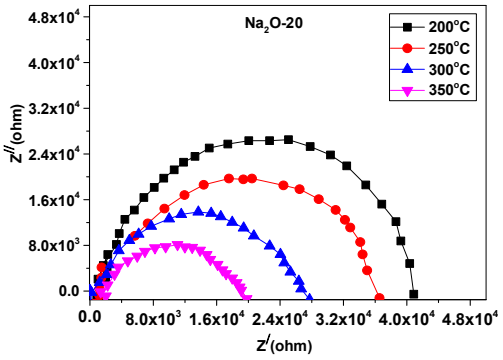

Fig.-5c: The Cole-Cole plots of Na_2O-20

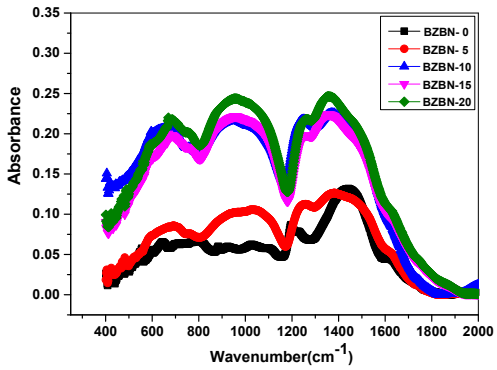

Fig.-6: The FT-IR Spectra of Na_2O Series

FTIR Spectra of Na_2O Enriched into Zinc-Barium-Borate Glasses

The BZBN glass series composition system exhibits a fixed Zn-O and Ba-O molar ratio of 10 molar percentage, a reduction in B_2O_3 molar concentration of 60% to 20%, and a rise in Na_2O molar percentage from zero to 20% with a 5% molar ratio increment. FTIR spectra of the BZBN glass series are displayed in Fig.-6 and the de-convoluted spectra are given in the Fig.-7. The band locations in this composition spectrum of BZBN glass series were found in the following regions: 393–410 cm^{-1}, 503–518 cm^{-1}, 790-810 cm^{-1}, and 2800-2904cm^{-1}.[10] B_2O_3-ZnO-BaO-Na_2O glass samples were subjected to FTIR measurements at room temperature using an FTIR spectrophotometer, with a measurement range of 400 to 4000 cm^{-1}. The FTIR spectra of this series show a peak of about 798 cm^{-1} wavenumber region, which corresponds to the peak of the tetrahedral BO_3 units. One more peak was seen at about 1240cm^{-1}, indicating the asymmetric stretching vibrations of ortho and pyro borate. Around the 710cm^{-1} wavenumber region that corresponds to the peak of the B-O-B bond bending vibrations, another peak emerged. The peak at about 400cm^{-1}, corresponds to the Na-O bond's bending vibrations.[11]

Table-1: FTIR Band Positions of (80-x) B_2O_3-10ZnO-10BaO-xNa_2O System

Bands	Assignment
393-410cm^{-1}	Vibrations of Na-O tetrahedral (Na_2O).
503-518cm^{-1}	Bending vibrations of BO_3 structural units
790-810 cm^{-1}	Bending vibrations of B–O–B in BO_4 units
1235-1241 cm^{-1}	Stretching vibrations of pyro and ortho units from borate groups.
2800-2904 cm^{-1}	H–O–H groups.

The Optical Absorption- Spectroscopic Analysis and its Features

In the optical absorption spectra of the glass system xNa_2O-10ZnO-10BaO-(80-x)B_2O_3 there is an appearance of a sharp absorption edge for all the glass specimens of BZBNa system as shown in Fig.-8. It confirms the characteristic behavior and nature of an amorphous material. The detection and shifting of the sharp absorption edge, towards the higher values of wavelengths with an increasing concentration of Na_2O. The cut-off value of the pure sample is 314nm and it is enhanced with an addition of the glass matrix transforming modifier oxide Na_2O as a linear trend.[12] Further, the addition of Na_2O results in the highest cut-off wavelength at 367 nm. In this case, only two network modifiers play the role with glass former B_2O_3. The non-bonding oxygen population will be increased as a function of modifier addition which leads to more randomness in the glass system. At the same time, the metal-oxygen-metal linkages will be formed in the glassy structure.[13] It also leads to the deformation of bonds and results in NBO creation along with lowering the rigidity of the structure. The values of the indirect band gap of the BZBNa glass system were calculated from Fig.-9 and it decreased from 3.93 eV to 3.75 eV when Na_2O content rose in the network. It occurred because of the growth of non-bridging oxygens. The optical band gap energy detected the lowest (3.75eV) for the pure BZBNa-0 sample. The values of cut-off based and other parameters of the BZBNa series are given in Table-2. The direct bandgap calculated values were gradually decreased. The variations found in the direct bandgap were 4.02 to 3.42 eV. The pure sample without Na_2O has shown the lowest value of refractive index. It was increased with the further addition of Na_2O mole fractions. The variation found in the refractive index is 2.12 to 2.26. It is purely an attribution

of the NBOs in the amorphous glass structure. The Urbach energy (ΔE) is the lowest for pure BZSNa-0 sample and it was raised with the addition of network modifying oxides which causes the creation of more disorderness or defect density in the form of NBOs. The range of ΔE lies between 0.42 and 0.80eV with the increase of Na_2O mole percentage. The breakage of bonding between the atoms may result in the conversion of tetra BO_4 to trigonal BO_3 units may occur when Na_2O is added to the glass network. The NBOs lead entire responsibility in the enhancement of the randomness of the glass network.[13] The Urbach energy variations are shown in Fig.-10.

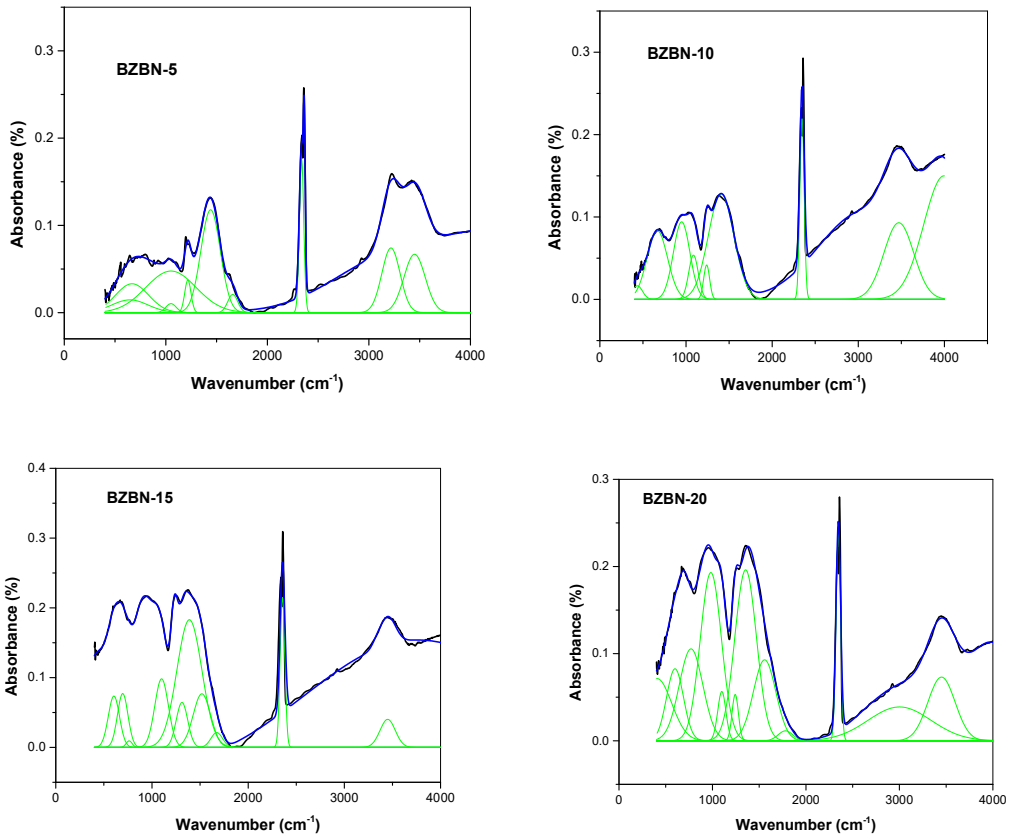

Fig.-7(a-d): The De-convoluted FT-IR Spectra of Na_2O Incorporated Borate Glass Series

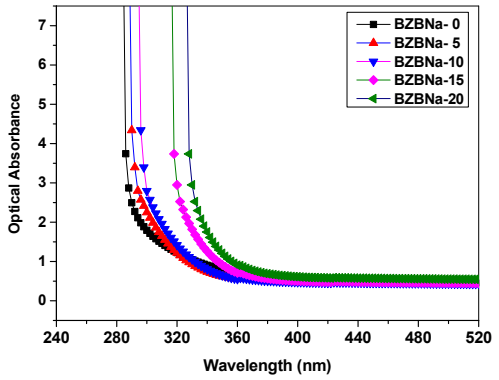

Fig.-8: The Variations in cut-off from Optical Spectra

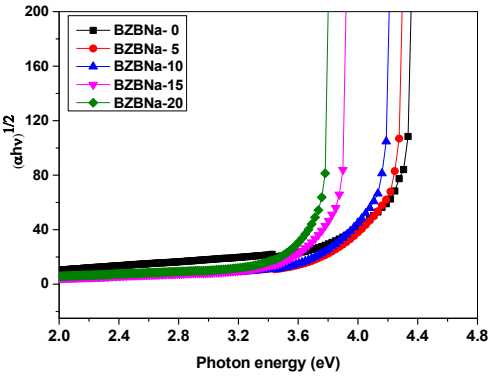

Fig.-9: Indirect Band Gap Calculation

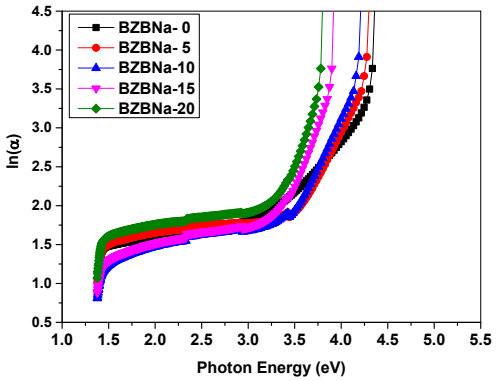

Fig.-10: The Variations in Urbach Energy

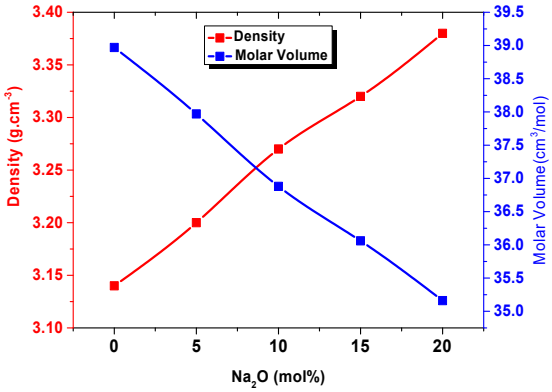

Fig.-11: Density Variations of BZBNa Series

Table-2: Optical/Physical Characteristics of BZBNa Glass System

Properties	BZB Na-0	BZB Na-5	BZB Na-10	BZB Na-15	BZB Na-20
The exp. density ($g.cm^{-3}$)	3.14	3.20	3.27	3.32	3.38
Molecular weight ($g.mol^{-1}$)	122.39	121.50	120.62	119.74	118.86
Molar volume ($cm^3.mol^{-1}$)	38.97	37.97	36.88	36.06	35.16
OPD ($g.atm.1^{-1}$)	66.70	65.83	65.05	63.77	62.56
Cut-off wavelength (nm)	314	325	338	358	367
Indirect band gap (eV)	3.95	3.78	3.62	3.43	3.36
Direct bandgap energy (eV)	4.05	3.84	3.70	3.52	3.42
Urbach energy (eV)	0.42	0.54	0.63	0.72	0.80
Molar refraction(cm^3mol^{-1})	23.46	22.18	21.02	20.16	18.15
Refractive index	2.12	2.15	2.17	2.22	2.26

Density characteristics of Na_2O glasses

Figure-11 reflects the variations in density (ρ) and molar volume (V_m) with the molar fraction of Na_2O increment. The density of the pure sample was found to be 3.14 $g.cm^{-3}$, in which the alkali modifier Na_2O content is zero, further, it was increased as the fraction of the additive content up to 3.38 g.cm-3. Generally, alkali oxide Na_2O entry into the borate network results in the transformation of units from BO_3 trigonal units to tetrahedral BO_4 units. The increment trends of the density of the current study can be assigned to the molar mass or molecular weights of the modifier oxides and also glass-forming oxide. The molecular weights of the oxides are Na2O-61.97 g.mol-1 and B_2O_3-69.63 $g.mol^{-1}$ respectively. The molar fractions of the B_2O_3 decrease, whereas, the lighter Na_2O replaces it in the existence of ZnO and BaO in the glass network. The NBOs are responsible for the trend of increasing density and it may also be due to the higher density oxides of BaO and ZnO.[14-17] It may also be due to the dependence on molar mass (M) and the ionic radius of the oxides present in the glassy structure. Basically, the V_m (molar volume) is decreased from 38.97$cm^3.mol^{-1}$ to 35.16cm^3mol^{-1} with the increase of Na_2O mole percentage. The density and molar volume of alkali (Na_2O) incorporated borate glasses showed an opposite trend. The present investigated glasses were shown a similar trend. The OPD varied from 66.70 to 62.56g.atm/l. The decreased values of the oxygen-packing-density revealed the void formation in the borate glass matrix and the generation of tetrahedral (BO_4) units in the glass networks and also an indication of the existence of NBOs with the substitution of alkali oxide Na_2O in place of B_2O_3. The overall results showed the enhancement of conductivity and optical properties compared to previous reports and also found that the present glassy materials are suitable for solid-state electrolytes.[18-20]

CONCLUSION

The newly developed glass series of the selected compositions were successfully synthesized by the melt-quench route. The AC conductivity enhancement is mainly due to cations like Na^+, $Zn^{+2,}$ and Ba^{+2} with applied frequency and also rising temperature. The highest conductivity of the present study was found in

the order of $10^{-3}\Omega^{-1}cm^{-1}$ at 350^0C. The overall improvement of conductivity is two orders. The highest Na_2O incorporated glass was shown the highest conductivity. The decreasing values of bulk resistance were found in the present study with an increase in temperature. The lowest order of bulk resistance was found as $10^4\Omega$. The FT-IR studies showed the presence of metal oxides with different vibrational modes and structural alterations. The results of optical spectra confirmed: an increase in cut-off and refractive index and a decrease in bond-gap energies. The density experiment proved the increase of density and decrease of molar volume. The enhanced properties of the studied glasses with excellent conductivity lead to their utility in battery and solid-state electrolyte applications.

ACKNOWLEDGMENTS

The authors must be thankful to the Head of, the Department of Chemistry for their support during the research work for the present study.

CONFLICT OF INTERESTS

The authors declare that there is no conflict of interest.

AUTHOR CONTRIBUTIONS

All the authors contributed significantly to this manuscript, participated in reviewing/editing, and approved the final draft for publication. The research profile of the authors can be verified from their ORCID IDs, given below:

Jagram Anterbedy http://orchid.org/0009-0007-5819-0002
Pallati Naresh http://orchid.org/0000-0003-3663-5940
Aravind Seema http://orchid.org/0009-0009-7854-6875
A.Rajesh http://orchid.org/0009-0001-2111-3894
K. Santosh Kumari http://orchid.org/0000-0002-2576-5742
Gangadhar Thalari http://orchid.org/0000-0002-5037-2609

Open Access: This article is distributed under the terms of the Creative Commons Attribution 4.0 International License (http://creativecommons.org/licenses/by/4.0/), which permits unrestricted use, distribution, and reproduction in any medium, provided you give appropriate credit to the original author(s) and the source, provide a link to the Creative Commons license, and indicate if changes were made.

REFERENCES

1. Ramesh Sopinti , Nagarjuna Gunnam , Bejjipurapu Chandrasekhar , Rajeswara Rao Darsi , G. Bhanu Kiran and Raghavaiah B.V, *Rasayan Journal of Chemistry*, **17(1)**, 47 (2024), http://doi.org/10.31788/RJC.2024.1718549
2. G.V. Jagadeesha Gowda, Bharath K Devendra, G. V. Ashok Reddy, G. Maruthi, M. Manjunatha,G. Harisha,C. Devaraja, *Rasayan Journal of Chemistry,* **16(2)**, 692 (2023), http://doi.org/10.31788/RJC.2023.1628300
3. N. Krishnamacharyulu, G. Jagan Mohini, G. Sahaya Baskaran,V. Ravi Kumar, N. Veeraiah, *Journal of Alloys and Compounds*, **734**, 318 (2018), https://doi.org/10.1016/j.jallcom.2017.10.271
4. J.S. Ashwajeet, T. Sankarappa, T. Sujatha, R. Ramanna, *Journal of Non-Crystalline Solids*, **486**, 52(2018), https://doi.org/10.1016/j.jallcom.2017.10.271
5. Al-Buriahi, M.S., Rashad, M., Alalawi, A.,Sayyed, M.I., *Ceramics International,* **46**,16452(2020), https://doi.org/10.1016/j.ceramint.2020.03.208
6. Bala, M., Agrohiya, S., Dahiya, S., Ohlan, A., Punia, R., Maan, A.S, *Journal of Molecular Structure*,**1219**, 128589 (2020), https://doi.org/10.1007/s12633-023-02832-6
7. Pallati Naresh, N. Narsimlu, Ch. Srinivas, Md. Shareefuddin, K. Siva Kumar, *Journal of Non-Crystalline Solids,* **49**, 120361(2020), https://doi.org/10.1016/j.jnoncrysol.2020.120361
8. M. Rajesh, M.R. Babu, N.J. Sushma, B.D.P. Raju, *Journal of Non-Crystalline Solids*, **528**, 119732(2020), https://doi.org/10.1016/j.jnoncrysol.2019.119732
9. Jamila S. Alzahrani, Andrei V. Lebedev, Samvel A. Avanesov, Alaa Hammoud, Z.A. Alrowaili, Zakaria M.M. Mahmoud, I.O. Olarinoye, M.S. Al-Buriahi, *Ceramics International,***48(13)**,18330 (2022), https://doi.org/10.1016/j.ceramint.2022.03.092

10. M. Vinoda Rani, Naresh Pallati, Ravi Kumar Vuradi, A. Sadananda Chary, S. Narender Reddy, *Journal of Non-Crystalline Solids*, **629**, 122862(2024), https://doi.org/10.1016/j.jnoncrysol.2024.122862
11. A. P. Shablinskii, S. N. Volkov, Bubnova, *Glass Physics and Chemistry,* **49**,709(2023), https://doi.org/10.1134/S1087659623600722
12. Mona Abo Zeed, R.M. El Shazly, E. Elesh, *Glass Physics and Chemistry,* **49**, 593(2023), https://doi.org/10.1134/S1087659623600400
13. Anjaiah, *Glass Physics and Chemistry,* **49**, 584 (2023), https://doi.org/10.1134/S1087659622600636
14. Yadong Lu, Xie, J., Guo, Y., *Glass Physics and Chemistry*, 49, 573 (2023). https://doi.org/10.1134/S1087659623600242.
15. M. J. Saadh, M. A. Mustafa, K. M. Batoo, *Ionics,* **30(5)**, 2657(2024), https://doi.org/10.1007/s11581-024-05440
16. M.R. Ahmed, K. Chandra Sekhar, S. Ahammed, V. Sathe, Z.A. Alrowaili, M. Amami, I.O. Olarinoye, M.S. Al-Buriahi, B.T. Tonguc, M. Shareefuddin, *Ceramics International*, **48**, 2124(2022), https://doi.org/10.1016/j.ceramint.2021.09.301 24
17. Swapna G. Upender, M. Prasad, *Journal of Taibah University of Science*, **11**, 583(2017), https://doi.org/10.1016/j.jtusci.2016.02.008 25
18. L. Griguta, I. Ardelean, *Modern Physics Letters B*, **21**, 1767(2007), https://doi.org/10.1142/S0217984907014152
19. S. Selvi, K. Marimuthu, G. Muralidharan, *Journal of Non-Crystalline Solids*, **461**, 35(2017), https://doi.org/10.1016/j.jnoncrysol.2017.01.028 7
20. C. Devaraja, G. V. Jagadeesha Gowda, B. Eraiah, *Journal of Alloys and Compounds,* **898**,162967 (2022), https://doi.org/10.1016/j.jallcom.2021.162967

[RJC- 8851/2024]